Geomagnetic induction and conductive structures in north-west India

B. R. Arora *Indian Institute of Geomagnetism, Colaba, Bombay 400 005, India*

F. E. M. Lilley and M. N. Sloane *Research School of Earth Sciences, Australian National University, Canberra, ACT 2600, Australia*

B. P. Singh *Indian Institute of Geomagnetism, Colaba, Bombay 400 005, India*

B. J. Srivastava and S. N. Prasad *National Geophysical Research Institute, Uppal Road, Hyderabad 500 007, India*

Summary. Magnetic disturbance events and quiet daily variation as recorded by the 1979 magnetometer array study in north-west India are analysed for evidence of electrical conductivity structures in the region. Contour maps of Fourier transform parameters are presented, and the disturbance event data are also reduced to sets of real and quadrature Parkinson arrows over a range of periods. A variety of conductive structures in the area are mapped, including some relatively shallow ones thought to be caused by sediments, as in the Ganga basin. More information is obtained on a major conductivity structure which strikes perpendicular to the Ganga basin into the foothills of the Himalayas; a second major conductivity structure is detected to lie to the west of the array area, and may be associated there with some aspect of the suture zone of India and Asia.

1 Introduction

An earlier paper (Lilley *et al.* 1981, hereafter called Paper 1) described the details of a magnetometer array which operated in north-west India in 1979, and was a collaborative exercise by the Indian Institute of Geomagnetism, the National Geophysical Research Institute of India and the Australian National University. The sites of the recording magnetometers of the array are shown again in Fig. 1 of the present paper for reference, and include the permanent observatories of Sabhawala, Jaipur and Ujjain. On the basis of analysis of a substorm polarized slightly west of north, Paper 1 reported preliminary results of an electrical conductivity anomaly striking at right angles to the Himalayan mountains, and noted the anomaly to be aligned with where the Aravalli belt would dip down under the
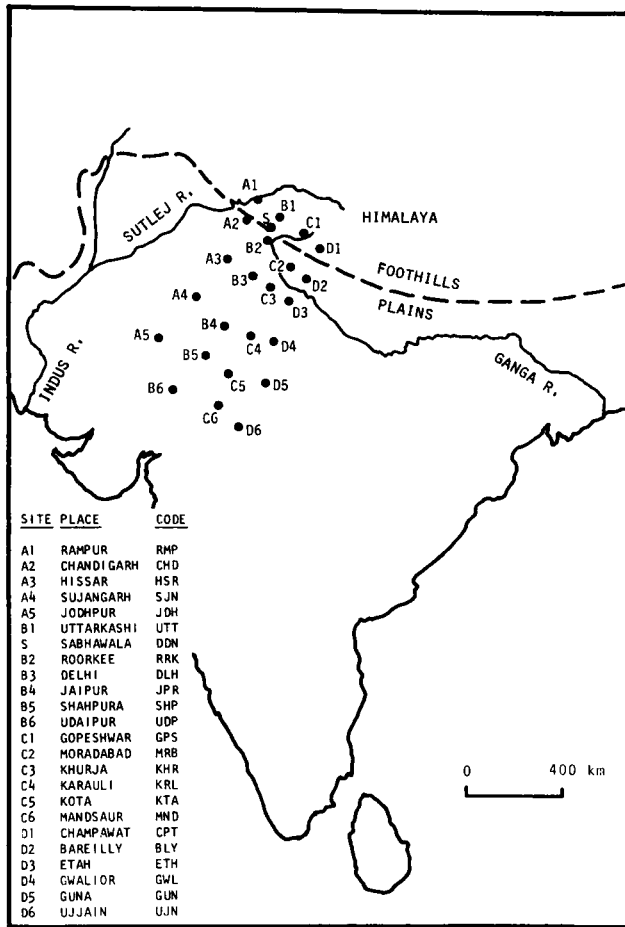
SITE	PLACE	CODE
A1	RAMPUR	RMP
A2	CHANDIGARH	CHD
A3	HISSAR	HSR
A4	SUJANGARH	SJN
A5	JODHPUR	JDH
B1	UTTARKASHI	UTT
S	SABHAWALA	DDN
B2	ROORKEE	RRK
B3	DELHI	DLH
B4	JAIPUR	JPR
B5	SHAHPURA	SHP
B6	UDAIPUR	UDP
C1	GOPESHWAR	GPS
C2	MORADABAD	MRB
C3	KHURJA	KHR
C4	KARAULI	KRL
C5	KOTA	KTA
C6	MANDSAUR	MND
D1	CHAMPAWAT	CPT
D2	BAREILLY	BLY
D3	ETAH	ETH
D4	GWALIOR	GWL
D5	GUNA	GUN
D6	UJJAIN	UJN

Figure 1. Observing sites for the 1979 magnetometer array in north-west India.

Ganga basin according to the tectonic model of the pre-Himalayan Indian plate under-thrusting the Asian plate upon collision.

The present paper now expands on Paper 1 and reports a more detailed analysis and synthesis of the north-west Indian array data. On the basis of digitized substorm events, a variety of sets of contour maps have been plotted of amplitude and phase Fourier transform parameters, and Parkinson arrows have been computed for anomalous responses in the vertical fluctuation component. To extend the information on geomagnetic induction in the area to long periods, a quiet day has been analysed and the patterns of its Fourier transform parameters are incorporated in the interpretation.

These further data sets confirm the position of the anomalous conductor determined in Paper 1, and also provide information on a number of other conductivity structures present in the area. At shorter periods the sediments of the Ganga basin contribute to complex electromagnetic induction effects, and at longer periods an anomaly to the west persists, interpreted as part of the suture zone of the Indian plate with Asia.

2 Basic data

2.1 SUBSTORMS

The results of the present paper are based on the six magnetic disturbance events listed in Table 1. These events were selected on the basis of their morphology, and the geographical distribution of those stations which recorded them. The events are polarized predominantly in the north-west sector but care was taken to ensure that disturbance-event induction was examined for as wide a range of horizontal polarizations as possible.

Fig. 2 presents stacked profiles for event 2. This event was selected because it was generally well-recorded by the northern stations of the array where, as demonstrated in Paper 1, initial inspection of the data showed strong anomalous effects to be present. Such anomalous effects are again clear in Fig. 2, where attention is drawn particularly to the variability of the vertical field profiles, Roorkee (B2) having a greatly enhanced vertical signal, as has also Etah (D3). The Etah (D3) signal is, however, reversed from that of Roorkee (B2), and other reversals are also evident: for example between Etah (D3) and Guna (D5), and then again between Guna (D5) and Ujjain (D6).

Of comparable significance are the differences in the horizontal-component fluctuations, the strongest of which are also evident on Fig. 2; especially the enhancements in the X- and Y-components at Gopeshwar (C1), Bareilly (D2), and Chandigarh (A2).

Event 2 in Fig. 2 has the most complicated morphology of the events analysed. Of the other events some profiles for events 1 and 3, and all recorded profiles for event 4, are given in Paper 1.

For technical reasons several hours of data only were recorded at Hissar (A3), however, the period recorded includes disturbances which were recorded simultaneously at the adjacent station Delhi (B3). Fig. 3 therefore presents the simultaneous events digitized for these two stations, and shows the reversal in the vertical fluctuation component (Z) which occurs between them. The occurrence of this reversal becomes basic evidence for the positioning of a conductive structure in the north-west part of the array, as discussed in Section 6.2 below.

For all substorm events, simultaneity of digitization is based upon the selection, in the X records, of some distinctive characteristic taken to have occurred simultaneously across the array area.

2.2 QUIET DAY

To examine geomagnetic induction in the array area at longer periods than is possible with substorm data, a quiet day was digitized, shown in Fig. 4. Digitization was carried out at

Table 1. Disturbance events digitized for analysis.

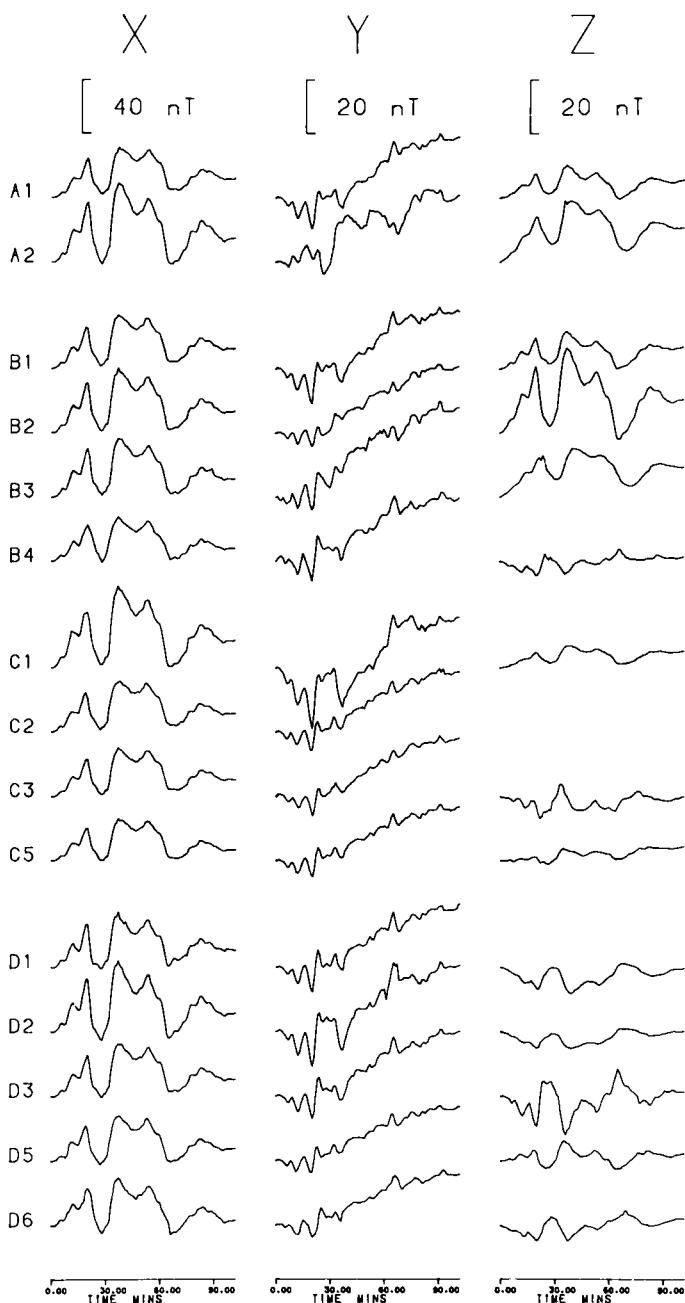| Event no.	Date (UT)	Approximate starting time (UT)	Duration (min)	Digitizing interval (min)
1	1979 April 2	1548 hr	88	2
2	1979 April 5	1559	102	1
3	1979 April 22	0605	60	2
4	1979 April 29	2054	110	2
5	1979 May 9	1848	118	2
6	1979 May 21	1828	126	2

Figure 2. Stacked profiles for the event of 1979 April 5. The notations *X*, *Y* and *Z* denote the magnetic fluctuation components in the directions of geographical north, east, and vertically downwards, respectively.

half-hourly intervals, simultaneity being based on the timing system of the recording instruments.

Fig. 4 shows typical *Sq* morphology characteristics of stations situated south of the northern hemisphere *Sq* focus path. Unlike the stacked profiles for the substorm event
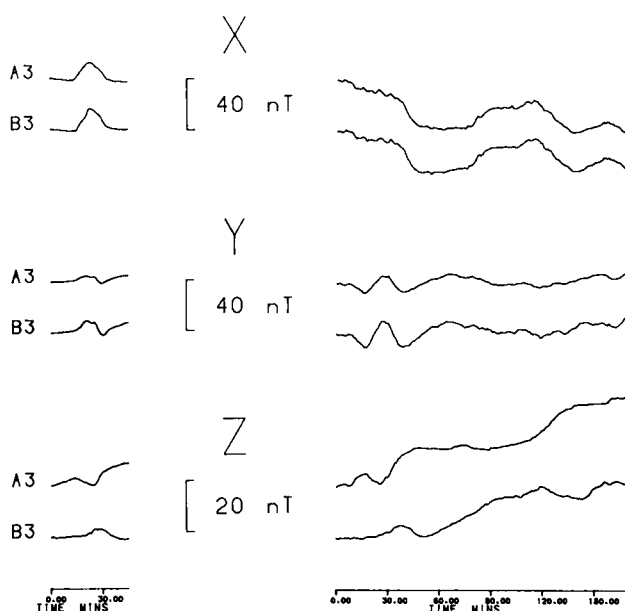
Figure 3. Simultaneous records for Hissar (A3) and Delhi (B3). The short event commenced at 0200 h UT on 1978 December 18 and the record shown is of duration 45 min. The long event commenced at 0720 h UT on 1978 December 18 and the record shown is of duration 2 hr 51 min.

shown in Fig. 2, the quiet day profiles in Fig. 4 are more uniform across the array area and do not show any obvious anomalies. This contrast between substorm and quiet-day profiles is due to two factors: first, source-field structures are different for substorms and quiet days, and the quiet-day source field causes the substantial normal (or non-anomalous) vertical (*Z*) fluctuations in Fig. 4. Secondly, and most significantly, the daily variation as a fluctuation of longer period penetrates deeper than the substorm fluctuations, and tends to 'filter out' the effects of more shallow conductive structures which may be exerting an appreciable influence on the substorm variations.

This latter factor, the deeper penetration or sampling of the daily variation source field, gives considerable importance to the records of Fig. 4. It is necessary to examine them more carefully, and in mapping their Fourier transform parameters as in Section 4 significant departures from their apparent uniformity become evident.

3 Data analysis

Generally, transformation to the frequency domain has been carried out according to the Fourier transform

$$g(\omega) = \int_{-\infty}^{\infty} f(t) \exp(-i\omega t)\, dt.$$

As in Paper 1, references to a cosine transform mean the real part of the transform as thus defined. In Paper 1 reference to a sine transform meant reference to the imaginary part of the transform; however, in this paper, for the sake of consistency with the usual definition of a sine transform, reference to a sine transform means the negative of the imaginary part
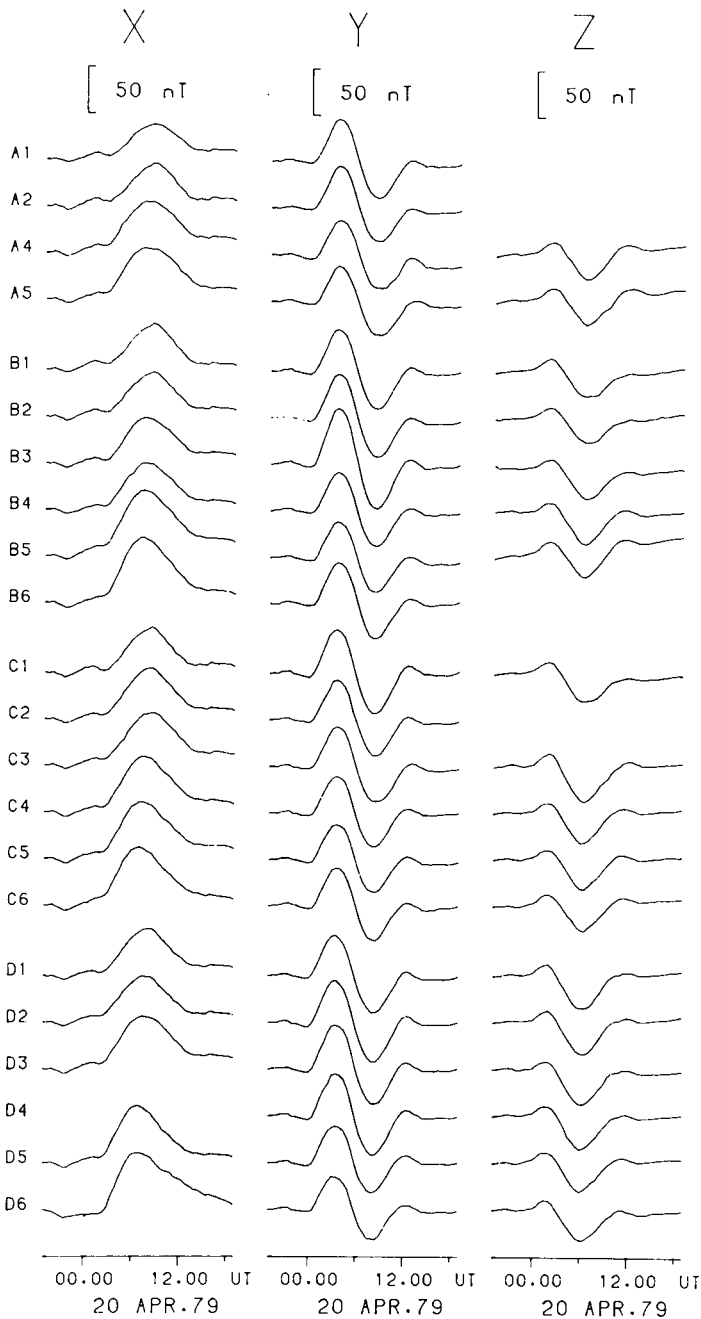
Figure 4. The magnetic quiet day of 1979 April 19–20 UT as recorded by the array. The records commence at 1900 h April 19 UT, which is 0030 h April 20 Indian Standard Time (IST) and so is close to local solar midnight for each station.

of the transform as defined above. Phases quoted are phase lags, in the sense that an event with a more positive phase value will have occurred at a later real time.

The events transformed have been generally chosen so that they can be examined physically complete and in isolation, without serious truncation of the time series involved.

The same transformation procedure has been applied to the quiet day of Fig. 4, based on the discussion of single quiet-day analysis given by Lilley (1975).

Before transformation, all records have had any differences between their first and last points removed as a linear trend. In some cases such a linear trend may be due to geomagnetic causes (as in Fig. 2 where the Y traces show the disturbance event of interest superimposed on the recovery phase of a larger storm) or, less often, instrumental effects (as in Fig. 4 where the Z trace for Shahpura, B5, shows drift caused by a recently-set Z sensor fibre).

4 Maps of Fourier transform parameters

4.1 SUBSTORMS

Some fifteen sets of contour maps have been drawn following the methods of Reitzel *et al.* (1970) for different periods and polarizations of the six disturbance events of Table 1. These sets of contour maps cover as wide a range of horizontal polarizations as possible, and span the period range of 8–91 min over which the spectra of the digitized events show adequate amplitude.

As might be expected from the complications of Fig. 2, the contour maps show a number of distinctive features. The most consistent of these features are displayed on the examples which now follow, and which supplement the single set of contour maps (for a north polarization at period 38 min) presented in Paper 1.
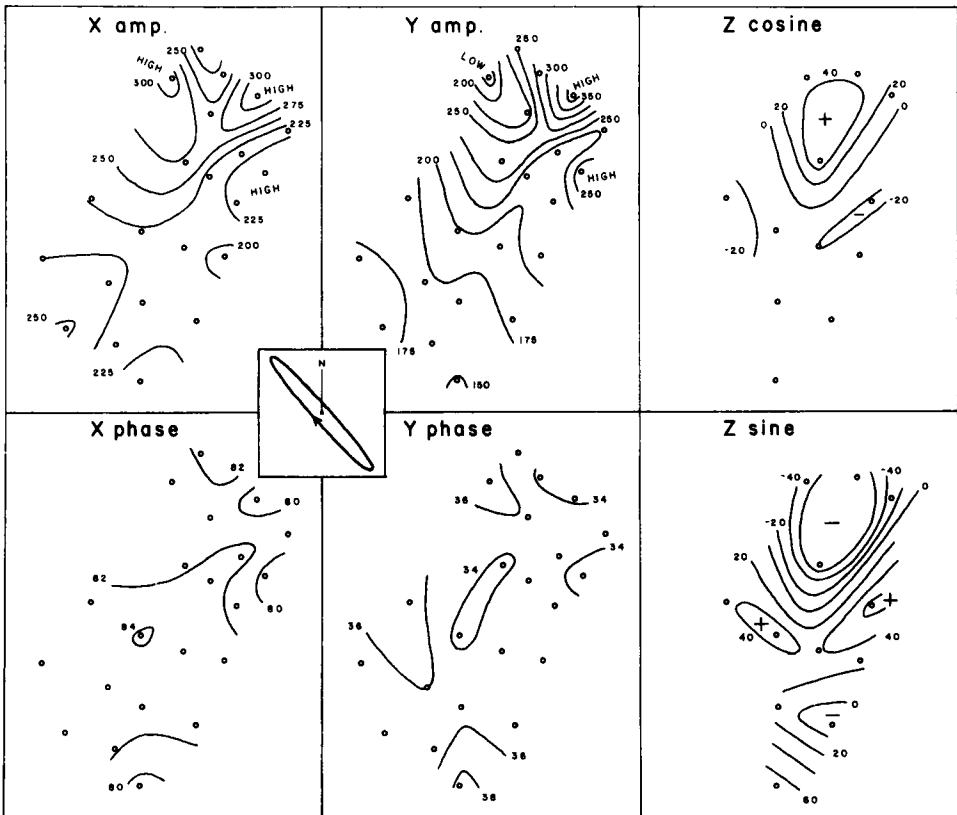

Figure 5. Contour maps of Fourier transform parameters and horizontal polarization ellipse for the event of 1979 May 9 at period 91 min.

The set of contour maps in Fig. 5 show the response of the area to a disturbance event polarized north-west. The period for which the maps have been plotted is 91 min, at the long-period end of the spectrum of the disturbance events examined. The north-west polarization should emphasize the conductor of Paper 1 by cutting across its strike, and indeed both vertical component Z cosine and Z sine maps in Fig. 5 show reversals in the northern part of the array. The horizontal component maps of Fig. 5 show, in the X amplitude, highs at Chandigarh (A2), Gopeshwar (C1) and Bareilly (D2); and in the Y amplitude, highs again at Gopeshwar (C1) and Bareilly (D2) but a low at Chandigarh (A2). The horizontal-component phase maps are typically featureless for north-west polarization.

Fig. 6 shows the response of the area to a disturbance polarized approximately north, at a period of 39 min. The polarization and period of this set of contour maps have been chosen for their similarity to those given in Paper 1, to emphasize the consistency of the main features of such contour maps for different events: the event of 1979 April 5 in Fig. 6, and the event of 1979 April 29 in Paper 1. The present Fig. 6 shows a more complicated reversal centred on station Khurja, C3 (the Z records for which were missing from the contour maps of Paper 1, and also from Fig. 5 above).

Regarding horizontal components, the north polarization of Fig. 6 produces the same amplitude patterns as the north-west polarization of Fig. 5 in both X- and Y-components, except that in the Y amplitude map the pattern at Chandigarh (A2) has changed from a low
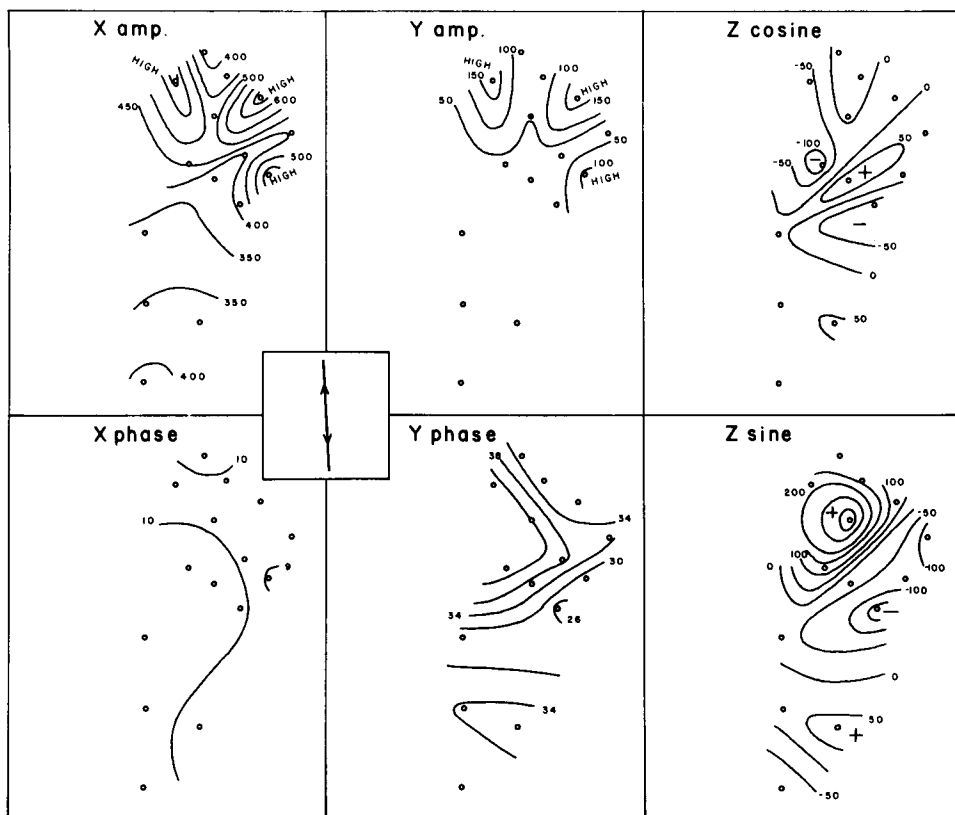

Figure 6. Contour maps of Fourier transform parameters and horizontal polarization ellipse for the event of 1979 April 5 at period 39 min.

in Fig. 5 to a high in Fig. 6. The change of polarization from Figs 5 to 6 also produces a distinctive pattern in the Y phase, to be interpreted below as correlating with the boundary of the sediments along the Himalayan foothills.

A return to a north-west polarization now at a much shorter period (8 min) is shown in Fig. 7, with data from the same event as Fig. 6 (the 1979 April 5 event shown in Fig. 2). In the vertical field component, the pattern is very similar to that of Fig. 6 (compare the Z sine pattern of Fig. 6 with the Z cosine pattern of Fig. 7, and vice versa); with again a reversal occurring on either side of Khurja (C3) in the Z sine map of Fig. 7.

In the horizontal fields, for the short period of Fig. 7 the three usual highs are present in the X amplitude map, but they have changed relative magnitudes so that the strongest is now at Bareilly (D2). This observation will be used below to link the Bareilly anomaly to a shallow feature. As for the north-west polarization in Fig. 5, in Fig. 7 the Y amplitude pattern at Chandigarh (A2) is low, and generally both X and Y phase patterns are featureless.

4.2 QUIET DAY

For the quiet day of Fig. 4, four sets of contour maps have been drawn for periods of 6, 8, 12 and 24 hr. The set for 12 hr is presented in Fig. 8, and is important as forming the basis for the response of the array area to 'long-period' inducing fields. The main features of Fig. 8 are as follows.
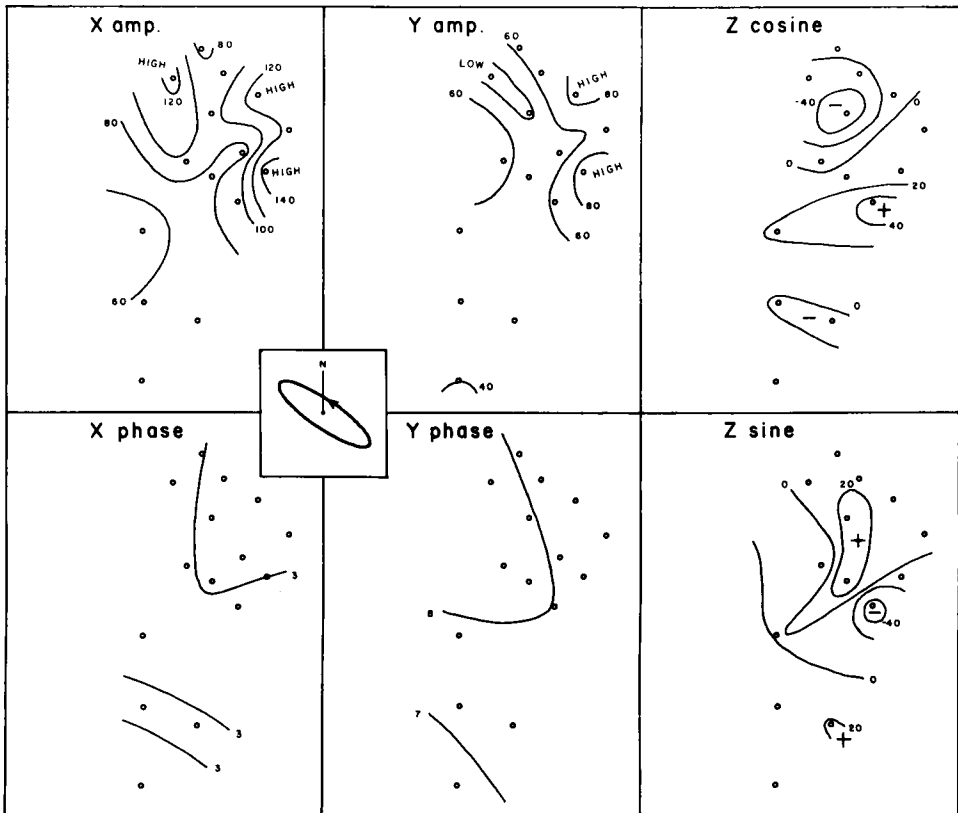

Figure 7. Contour maps of Fourier transform parameters and horizontal polarization ellipse for the event of 1979 April 5 at period 8 min.

17

4.2.1 Amplitude patterns

For simple quiet daily variation over a geology of horizontal layering, amplitude patterns consist of contour lines uniformly aligned east—west. In Fig. 8, however, there is a strong anomaly in the amplitude pattern of the Y component, and also a corresponding anomaly in the amplitude pattern of the Z component. This Z pattern coincides in position with the Z patterns of the substorm data in Figs 5, 6 and 7.

4.2.2 Phase patterns

The phase maps in Fig. 8 show an anomaly in the X component, and both X and Z components show general east—west gradients of about twice that which would be expected for motion of the source field with local solar time. The Y phase pattern does, however, show an east—west gradient approximately in agreement with that for local solar time, so that the anomaly in the Y amplitude is evidently in phase with the regionally induced normal current flow in the Earth.

5 Transfer functions and Parkinson arrows

After Fourier transformation, the substorm data for each station of the array have been analysed to determine their best fit to the equation
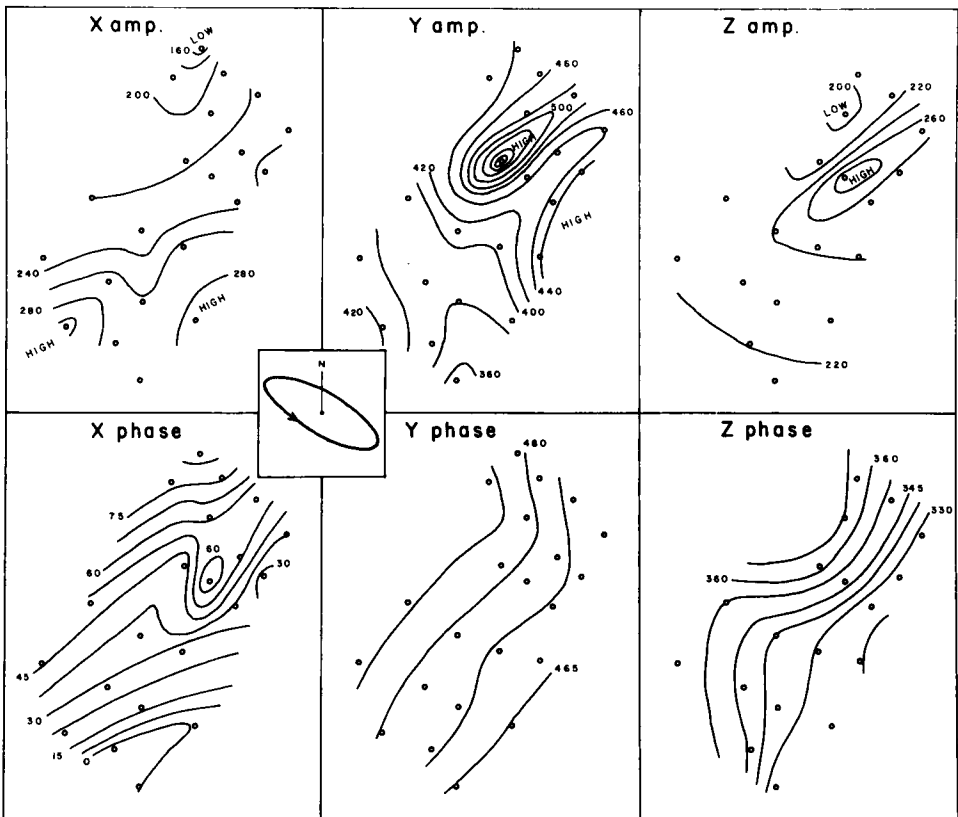
$$Z = AX + BY \tag{1}$$

Figure 8. Contour maps of Fourier transform parameters and horizontal polarization ellipse for the quiet day of 1979 April 19—20 at period 12 hr.
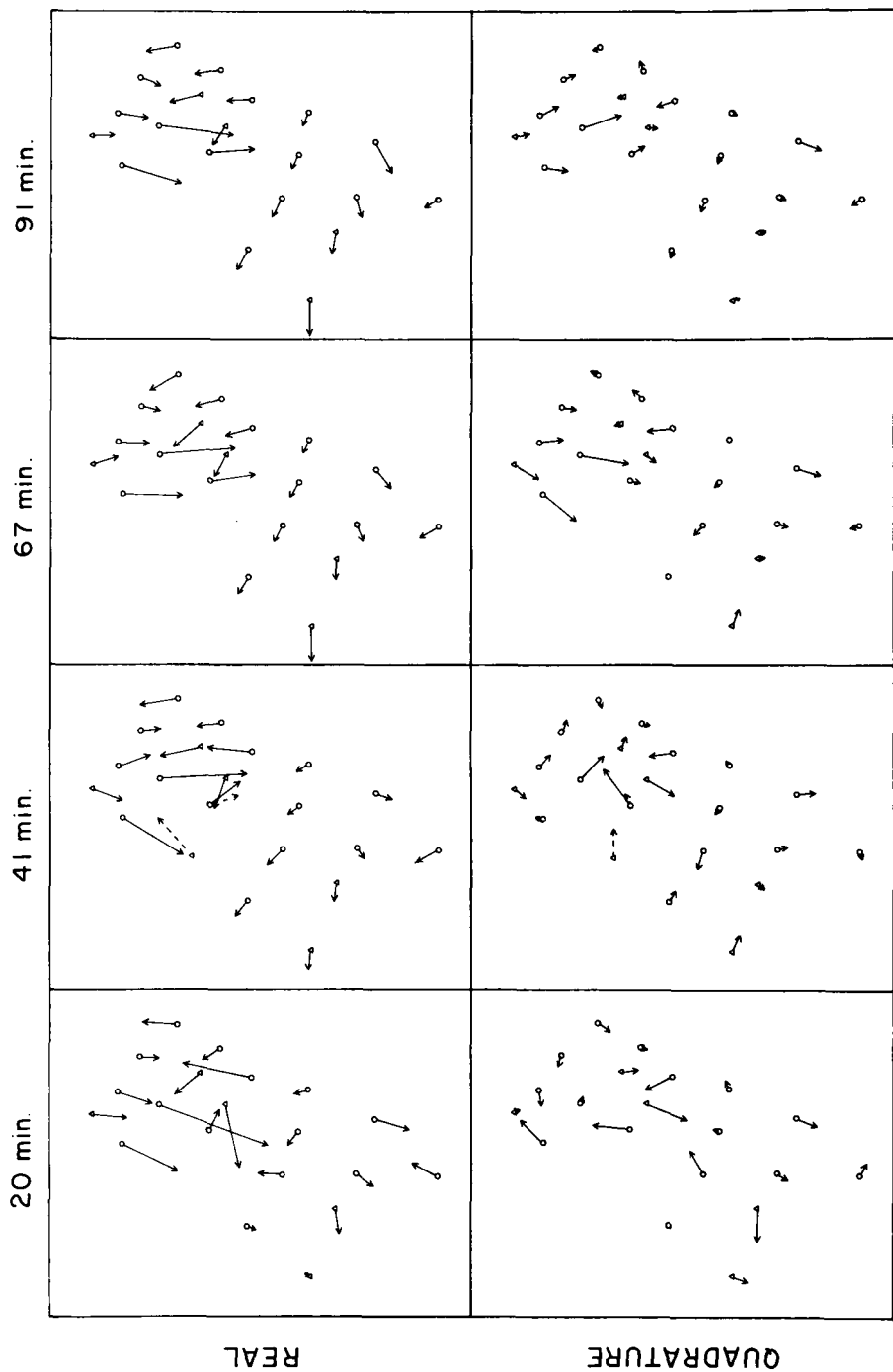
Figure 9. Real and quadrature Parkinson arrows for the stations of the north-west India magnetometer array, at four different periods. Triangles mark stations for which arrows have been determined on the basis of three disturbance events or less. For Hissar and Delhi at period 41 min the dashed arrows have been determined from the disturbance records shown in Fig. 3.

where A and B are (complex) constants, often termed 'transfer functions', for a particular site for a particular frequency of magnetic fluctuation. In the present work, such transfer functions for the array stations have been determined by two methods.

(1) By use of the standard cross-power and auto-power solution for equation (1) above, as given for example by Schmucker (1964, 1970) and Everett & Hyndman (1967). For the present data cross-power and auto-power estimates for a station were obtained by taking averages, over the events analysed, of the Fourier transform values for that station.

(2) By solving equation (1) above as an overdetermined linear set of simultaneous equations, constructed by imagining equation (1) to hold for every individual event (Woods 1979).

Both methods of data analysis produce comparable values for A and B, and in the customary way these values have been combined to form Parkinson arrows for the vertical field response, by drawing arrows with a component A to the south and B to the west, for both real and quadrature parts. Sets of such arrows are presented in Fig. 9, stepping in period from 20 to 91 min.

With simultaneous records for an array of stations there are various ways of choosing the normal X and Y signals to combine with the Z signal of a particular station in equation (1) above (see, for example, Gough & de Beer 1980). For the arrows of Fig. 9, the horizontal fields at Karauli (C4) were taken as the normal horizontal fields for all other stations, except for events 1 and 2 when the horizontal fields at Khurja (C3) and Kota (C5) respectively were used (Karauli not having recorded these events). Depending upon the number of events recorded, the number of events used in solving equation (1) varied from station to station.

The dashed arrows for Delhi (B3) and Hissar (A3) in the set for 41 min in Fig. 9 are 'single-station' induction arrows, evaluated using Fourier transforms of the disturbance events of Fig. 3 at five frequencies in the period interval 30–42 min. The combination of such transform information over a period range is made upon the basis that, over the range in question, the polarization characteristics of the geomagnetic events change more rapidly than do the A and B transfer functions of equation (1). Such use of a relatively rapid change in disturbance-event polarization characteristics was previously tested by Woods & Lilley (1979), and found satisfactory.

5.1 REAL ARROW PATTERNS

In the north-east corner of the array there is a reversal in the direction of the arrows, corresponding to the Z patterns seen in Figs 5, 6 and 7, between a group of stations consisting of Rampur (A1), Chandigarh (A2), Uttarkashi (B1), Roorkee (B2), Delhi (B3) and Gopeshwar (C1) on the one hand, and Moradabad (C2), Khurja (C3), Champawat (D1), Bareilly (D2) and Etah (D3) on the other. The line of this reversal is the main evidence for the position of a major conductive structure interpreted to exist below the array area.

In the southern half of the array the arrows systematically point west or north of west. There are other features shown only by individual stations, such as the reversal between Chandigarh (A2) and Hissar (A3) evident in the set of arrows for 41 min period, and at the shortest period shown of 20 min the reversal between Kota (C5) and Guna (D5), and Ujjain (D6).

5.2 QUADRATURE ARROW PATTERNS

The quadrature arrows in Fig. 9 also show the reversal in the north-east of the array, with the Rampur (A1), Chandigarh (A2), Uttarkashi (B1), Roorkee (B2) and Delhi (B3) arrows

at 91 min pointing generally south or east of south, and the Etah (D3) quadrature arrow pointing west of north. Otherwise the quadrature arrows are generally weak, especially in the southern half of the array: an observation that will be used to attribute the westward-pointing real arrows in the southern half of the array to a massive and highly conductive structure.

5.3 VARIATION WITH PERIOD

In Fig. 9, the most simple arrow patterns are those for the longest period shown, 91 min. As period decreases, Fig. 9 shows that the arrow patterns change in systematic ways. For example the real arrows in the Sujangarh (A4), Jaipur (B4), Karauli (C4) and Gwalior (D4) line all swing clockwise, due, it will be interpreted below, to the relatively stronger effect at short periods of the sediments of the Ganga basin to their north-east. The next line of stations to the south comprising Jodhpur (A5), Shahpura (B5), Kota (C5) and Guna (D5), swing systematically anticlockwise as period decreases and at period 20 min the real arrows at Guna (D5) and Ujjain (D6) have swung to oppose each other; implying their reversal too is due to a relatively shallow structure. An additional feature of the patterns is the real arrow at Etah (D3), which increases substantially in length as period decreases.

6 Physical interpretation

The array data have been examined in the three different forms of stacked profiles, contour maps, and arrow patterns. The main anomalous features noted are consistent between the different ways of data presentation, and will now be used to build a map of electrical conductivity structures in the area studied. Several general principles will be followed in this interpretation.

(1) Parkinson arrows will be taken to generally point towards conductive structures, or to the higher conductivity side of electrical conductivity contrasts.

(2) Real arrows strong compared to quadrature arrows which accompany them will be taken to be caused by structures of primarily reactive inductive response, such as massive and possibly deep highly conductive bodies, in which induced fields are closely in-phase with their inducing fields. Real arrows accompanied by quadrature arrows of comparable magnitude, however, will be taken to be caused by less massive conductors of more resistive inductive response, such as surface sediments, in which a marked phase difference occurs between induced and inducing fields.

(3) On the basis of electromagnetic skin-depth considerations, substorm data will be taken to reflect the electrical conductivity structure at crustal depths, the daily variation penetrating, however, well into the mantle.

The features noted in the fluctuations patterns for the area may then be accounted for by two major 'first-order' conductivity structures, marked I and II on Fig. 10, supplemented by four minor or 'second-order' conductivity structures, marked III, IV, V and VI on Fig. 10. These structures, from a physical point of view, are as follows.

6.1 FIRST-ORDER CONDUCTIVITY STRUCTURES

(I) The line of current flow of Paper 1 is now confirmed as a major conductivity structure. In addition to the evidence for it from the substorm contour maps and arrow patterns, its effect is also evident in the long-period data of Fig. 8, which are otherwise clear of the anomalous features seen in the shorter period data of Figs 5 to 7.
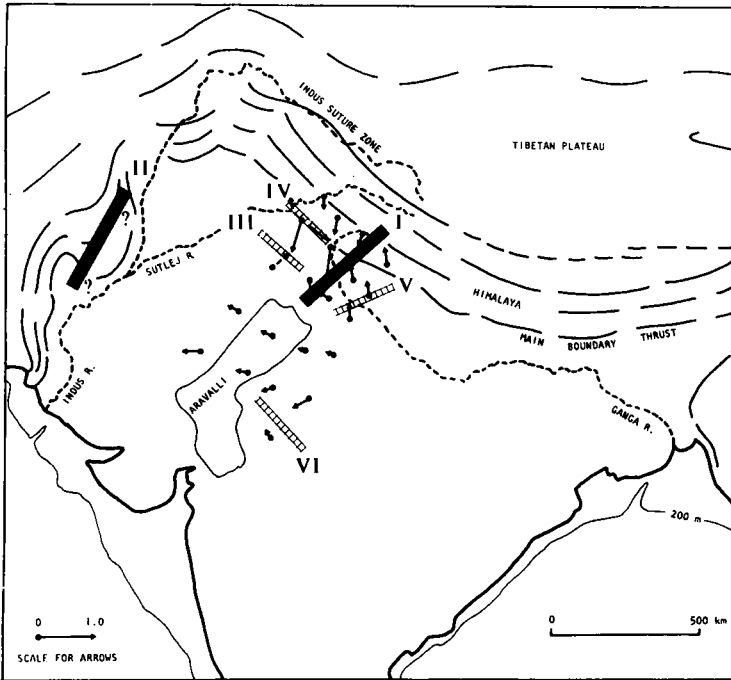
Figure 10. Map of India, showing interpreted conductive structures superimposed on the real Parkinson arrows for 91 min from Fig. 9 (the dashed arrow for Hissar, A3, is for 41 min). Question marks beside the conductive structure II emphasize the speculative nature in the positioning of this structure. Structures I and II are classed as 'first-order', and structures III to VI are classed as 'second-order'.

(II) A conductor to the west of the array is indicated by the westward-pointing real arrows in the southern half of the array in Fig. 9. That the quadrature arrows for the same stations are negligibly small is taken to indicate that the real arrows are due to induction in a massive structure of high electrical conductivity. If this structure is exerting a sufficiently strong influence, then its position could be up to hundreds of kilometres distant from the observing stations: the situation may be similar to the case in southern Africa where Gough, de Beer & van Zijl (1973) have determined smooth patterns over horizontal distances of hundreds of kilometres for real arrows of periods comparable to those of Fig. 9, and have attributed this consistency of arrow direction primarily to the effect of a large conductive body under the Cape Fold Belt (termed the Southern Cape Conductive Belt in the subsequent enlarged array study by de Beer & Gough 1980).

6.2 SECOND-ORDER CONDUCTIVITY STRUCTURES

(III) The reversal in the vertical-field component shown in Fig. 3 between Hissar (A3) and Delhi (B3), and the reversal in Parkinson arrows shown in Fig. 9 for period 41 min between Hissar (A3) and Chandigarh (A2), are taken to indicate an electrical conductivity structure approximately in the position marked III in Fig. 10.

(IV) The dependence on horizontal-field polarization of the relative Y amplitude strengths at Chandigarh (A2) and Rampur (A1), and the Y phase pattern for north polarization shown particularly in Fig. 6, are taken to indicate an electrically conductive structure in the position marked IV in Fig. 10.

(V) The relative predominance of the horizontal field amplitudes at Bareilly (D2) as period decreases, coupled with the associated increasing magnitude of the real Parkinson arrow for Etah (D3), and the structure of the Z cosine pattern in Fig. 6 (seen again in the Z sine pattern of Fig. 7): these features are interpreted by a shallow conductor marked V in Fig. 10.

(VI) The reversal in Parkinson arrows in Fig. 9 between Guna (D5) and Ujjain (D6) at period 20 min is interpreted by a shallow conductor running between them, marked VI on Fig. 10.

7 Geological interpretation

The conductive structures marked in Fig. 10 on the basis of the physical interpretation of the previous section have the following geological connotations.

7.1 FIRST-ORDER FEATURES

(I) As noted in Paper 1 the structure has a position and orientation appropriate for it to be part of the Aravalli belt, given that from its area of outcrop this belt continues north-east under the Ganga basin to dip down under the foothills of Himalayas, at the Main Boundary Thrust fault. The conductivity structure coincides in position with the seismically active Delhi-Hardwar Ridge (Kaila & Narain 1976) and also with a gravity feature which protrudes out from a gravity pattern otherwise predominantly following the strike of the Himalaya Mountains (Qureshy 1969).

The agreement in position of the basement ridge, the seismicity, the gravity anomaly and the electrical conductivity structure is interpreted as indicating localized tectonic activity in this part of the Indian plate as it dips below the Himalayas. A model is visualized in which stresses associated with the underthrusting processes are causing the plate to fracture, allowing intrusion upwards of magma from the asthenosphere beneath.

(II) The 'western conductor', not suspected in Paper 1, is a strong conductivity feature now evident from the present study. Observations at more stations further west are needed to determine its position, but the speculation is advanced in this paper that it is associated with the great shearing along the Chaman Fault that occurred and is still occurring as a consequence of the collision of India with Asia. The effect of sediments in the Indus valley have also to be clarified in the complete interpretation of this western conductor.

7.2 SECOND-ORDER FEATURES

(III and IV) The sediments of the Ganga basin may be expected to have a strong effect on magnetic fluctuations in northern India. Given the physical evidence in Section 6.2 for the general positions of the conductivity features III and IV, in actually drawing them in on Fig. 10 guidance has been taken from the known extent of the Ganga basin. Line IV runs along the foothills of the Himalayas, to the south of which sediments reaching a thickness of 4–6 km have been inferred from aeromagnetic data (Mathur & Kohli 1963). Line III marks the southern boundary of the Indo-Gangetic plains. On the basis of aeromagnetic and gravity data, a rise in basement topography underneath structure III has been suggested by Sen Gupta (1964) and Warsi & Molnar (1977).

(V) Structure V follows a trough in the sediments of the Ganga basin bounded by the Delhi-Hardwar ridge on the west and the Moradabad fault to the east.

(VI) Structure VI appears to be correlated with the sediments of the Godavari valley, which has been suggested by Qureshy *et al.* (1968) on the basis of gravity data to extend up to the south-east corner of the array area.

8 Conclusions

The array experiment has been successful as a reconnaissance study of geomagnetic induction patterns reflecting electrical conductivity structure in north-west India. Above the Ganga basin induction effects are complex and change over a short distance, so that follow-up work with instruments spaced more closely is needed to clearly define the near-surface induction effects taking place in sediments. The main result of Paper 1 is confirmed, that a conductor strikes across the Ganga basin into the Himalayan foothills, causing reversals in the vertical component of substorm fluctuations and affecting also the pattern of the magnetic quiet daily variation.

In contrast with induction above the Ganga basin, the pattern over the southern part of the array is more uniform. Real Parkinson arrows for period 91 min point generally west, possibly to a high conductivity structure at the suture zone of India and Asia.

It may be valuable in conclusion to add some notes on how the results of the present paper might be carried further ahead. Closer station spacing is especially desirable for the zones of anomalous magnetic fluctuation, and also to the west of the present array area to clarify the position of the 'western conductor'. With the reconnaissance work now achieved, such closer station spacing might be carried out with fewer instruments than a whole array. Magnetotelluric soundings would provide valuable complementary information, and sounding sites can be planned with the conductive structures of the present array study in mind.

Interpretation of the conductivity structures quantitatively may be expected to be difficult, especially as the anomaly crossing the Ganga basin causes a 'three-dimensional' situation and the character of induction taking place further into the mountains is not known. One benefit is that the gross structure of the sediments is reasonably well known, for the purposes of specifying the sediments in a model. A key question to be decided, however, is the extent to which the anomalous currents observed are induced locally, or are part of a larger global system, linked to the oceans.

References

De Beer, J. H. & Gough, D. I., 1980. Conductive structures in southernmost Africa: a magnetometer array study, *Geophys. J. R. astr. Soc.,* 63, 479–495.
Everett, J. E. & Hyndman, R. D., 1967. Geomagnetic variations and electrical conductivity structure in south-western Australia, *Phys. Earth planet. Int.,* 1, 24–34.

Gough, D. I. & de Beer, J. H., 1980. Source field bias in geomagnetic transfer functions: a case history, *J. Geomagn. Geoelect., Kyoto*, **32**, 471–482.

Gough, D. I., de Beer, J. H. & van Zijl, J. S. V., 1973. A magnetometer array study in southern Africa, *Geophys. J. R. astr. Soc.*, **34**, 421–433.

Kaila, K. L. & Narain, H., 1976. Evolution of the Himalaya based on seismotectonics and deep seismic soundings, *Proc. Himalayan Geol. Sem. Section II: Structure, tectonics, seismicity and evolution*, pp. 1–30.

Lilley, F. E. M., 1975. The analysis of daily variations recorded by magnetometer arrays, *Geophys. J. R. astr. Soc.*, **43**, 1–16.

Lilley, F. E. M., Singh, B. P., Arora, B. R., Srivastava, B. J., Prasad, S. N. & Sloane, M. N., 1981. A magnetometer array study in northwest India, *Phys. Earth planet. Int.*, **25**, 232–240.

Mathur, L. P. & Kohli, G., 1963. Exploration and development for oil in India, *Sixth World Petrol. Congr., Sect. 1, Paper 25*.

Qureshy, M. N., 1969. Thickening of a basalt layer as a possible cause for the uplift of the Himalayas – a suggestion based on gravity data, *Tectonophys.*, **7**, 137–157.

Qureshy, M. N., Krishna Brahman, N., Garde, S. E. & Mathur, B. K., 1968. Gravity anomalies and Godavari Rift, India, *Bull. geol. Soc. Am.*, **79**, 1221–1230.

Reitzel, J. S., Gough, D. I., Porath, H. & Anderson, C. W., 1970. Geomagnetic deep sounding and upper mantle structure in the western United States, *Geophys. J. R. astr. Soc.*, **19**, 213–235.

Schmucker, U., 1964. Anomalies of geomagnetic variations in the south-western United States, *J. Geomagn. Geoelect. Kyoto*, **15**, 193–221.

Schmucker, U., 1970. Anomalies of geomagnetic variations in the southwestern United States, *Bull. Scripps Instn Oceanogr. No. 13*.

Sen Gupta, S., 1964. Possible subsurface structures below the Himalayas and the Gangetic plains, *Proc. 22nd Int. Geol. Congr.*, Sect 11, 334–352.

Warsi, W. E. K. & Molnar, P., 1977. Gravity anomalies and plate tectonics in the Himalaya, in *Ecologie et Geologie de l'Himalaya, Colloques int. Cent. Natn Rech. scient.* No. 268, 463–477.

Woods, D. V., 1979. Geomagnetic depth sounding studies in central Australia, *unpublished PhD thesis*, Australian National University, Canberra.

Woods, D. V. & Lilley, F. E. M., 1979. Geomagnetic induction in central Australia, *J. Geomagn. Geoelect., Kyoto*, **31**, 449–458.